

TeAAL: A Declarative Framework for Modeling Sparse Tensor Accelerators

Nandeeka Nayak*, Toluwanimi O. Odemuyiwa**, Shubham Ugare*, Christopher Fletcher*, Michael Pellauer†, Joel Emer†‡
*University of Illinois–Urbana Champaign, **University of California–Davis, †NVIDIA, ‡Massachusetts Institute of Technology
{ndnayak2, sugare2, cwfletch}@illinois.edu, todemuyiwa@ucdavis.edu, {mpellauer, jemer}@nvidia.com

Abstract—Over the past few years, the explosion in sparse tensor algebra workloads has led to a corresponding rise in domain-specific accelerators to service them. Due to the irregularity present in sparse tensors, these accelerators employ a wide variety of novel solutions to achieve good performance. At the same time, prior work on design-flexible sparse accelerator modeling does not express this full range of design features. This has made it difficult to compare or extend the state of the art, and understand the impact of each design choice.

To address this gap, we propose TeAAL: a framework that enables the concise and precise specification and evaluation of sparse tensor algebra architectures. We use TeAAL to represent and evaluate four disparate state-of-the-art accelerators—ExTensor [14], Gamma [50], OuterSPACE [29], and SIGMA [34]—and verify that it reproduces their performance with high accuracy. Finally, we demonstrate the potential of TeAAL as a tool for designing new accelerators by using it to propose a novel accelerator for the sparse MTTKRP kernel.

I. INTRODUCTION

Sparse tensor algebra workloads have exploded in popularity over the past few years. For example, the two most computationally intensive operations required for deep learning are matrix multiplication and convolution, both of which—due to the prevalence of ReLU for non-linearization and the explicit pruning of filter weights [4], [24], [42]—may act on sparse tensors, i.e., tensors with many zeros. However, many other applications process sparse data, including graph algorithms [3], [5], [11], [25], [28], [39] and physical simulations [17], [43], [45]. This surge has been accompanied by a corresponding rise in proposals for custom hardware to service them [13], [14], [29], [31], [34], [50], [51]. While these accelerators have the potential to provide dramatic speed-ups over the best CPU and GPU algorithms, they take significant effort and space to describe, refine, and evaluate.

There are a number of tools that support the concise specification and modeling of accelerators targeting tensor computations operating on dense tensors [30], [49]. To simplify specification [35], these tools allow the user to separately provide a target *algorithm* (i.e., a functional description of the problem, such as an equation in Einstein summation (Einsum) notation [12]) and a *mapping*, which describes when and where in the processor each action (e.g., compute or storage access) occurs [7]. These, together, correspond to a *mapped representation* (e.g., a loop nest) which describes both the algorithm and how it is executed. The mapped representation is then evaluated by a *model of the target platform* to produce efficiency metrics, like performance and energy.

At the same time, the above level of tool support does not yet exist for modeling accelerators operating on sparse tensors. Non-uniform, input-dependent sparsity necessitates specialized algorithms and mechanisms to cope with the irregular (often low) data reuse, myriad compression formats, additional meta-computation (e.g., intersection), and more. Therefore, tools targeting dense tensor computations cannot accurately model the work performed by architectures targeting sparse tensor kernels.

Furthermore, different designs have used a variety of different mechanisms to cope with sparsity — even when targeting the same problem. For example, SIGMA [34], a sparse-matrix sparse-matrix multiplication (SpMSPM) accelerator, achieves high utilization of its PE array by filling the array with only non-zero elements, regardless of the coordinates they correspond to. As another example, OuterSPACE [29] splits SpMSPM into several phases that respectively produce, sort, and consume an array of linked lists representing partial products. Gamma [50] exploits yet a third strategy: executing the kernel with Gustavson’s algorithm and using a high-radix hardware merger to do so efficiently.

Existing tools for modeling sparse tensor algebra accelerators are not expressive enough to support this diversity. For example, STONNE [27] supports only the monolithic SpMSPM kernel on a fixed accelerator topology. While this is sufficient to model SIGMA, it is unable to express either OuterSPACE or Gamma. Sparseloop [48] can model generic Einsums, but can only express one Einsum at a time. As we will see in Sections III and V, multiple Einsums are required to express SIGMA, OuterSPACE, and Gamma. Furthermore, neither framework has the ability to model operations like merging or sorting.

This work. Our key contribution is to show that recent sparse tensor algebra accelerators can be expressed as cascades (DAGs) of mapped Einsums, where computation and data movement (within and across Einsums) is expressed as a small set of primitive operations on tensors in the format-agnostic *fibertree* [42] representation. In doing so, we find that there are many instances of seemingly disparate design decisions mapping to singular core ideas (e.g., SIGMA’s work distribution strategy to fibertree rank flattening and OuterSPACE’s sort and Gamma’s merge into fibertree rank swizzling). This small set of core ideas can be combined in different ways to represent the variety in real-world accelerators. Then, to

realistically model performance, specific accelerators manifest as a combination of operations on fibertrees and a lowering of those fibertrees onto specific compressed representations (e.g., CSR) and hardware structures (e.g., buffers).

We realize the benefits of this approach by proposing TeAAL (for *Sparse Tensor Algebra Accelerator Language*), a novel framework for the precise design specification and modeling of sparse tensor algebra accelerators. By supporting both static and dynamic manipulations of fibertrees, TeAAL expresses more previously proposed accelerators than any prior work and enables a wider design space through which to search for future accelerators. The TeAAL specification language is a modular, declarative language that breaks computations up into a set of equations (Einsums) and a mapping that expresses the required processing and data movement as operations on fibertrees. TeAAL represents the model of the target platform with descriptions of the formats of each of the tensors, the architecture of the accelerator, and the binding of fibertree operations onto hardware structures. Once specified in TeAAL, our framework compiles the accelerator into an executable program that can be run on provided benchmark data to model efficiency.

Although attributes such as language expressivity and conciseness are difficult to quantify, as part of a study to validate TeAAL’s fidelity, we are able to write the TeAAL Einsum and mapping specifications of four recent (and disparate) sparse tensor algebra accelerator proposals (OuterSPACE [29], ExTensor [14], Gamma [50] and SIGMA [34]) in less than a page (see Figures 3 and 7), with each specification taking ~ 30 lines to represent. When the models generated for each of these accelerators were evaluated, they were able to reproduce the results for each architecture as reported in the original papers describing the accelerators.

TeAAL fills two crucial niches within the field of sparse tensor algebra accelerator design. First, it allows architects to compare more complex designs than current tools in an apples-to-apples fashion and understand the pros and cons of each. Furthermore, it allows architects to iteratively propose and evaluate accelerator designs. In this work, we perform such a design process for a sparse MTTKRP (the key computational kernel required for canonical polyadic decomposition (CPD) [41]) accelerator—and achieve a speedup over all prior work on SpMTTKRP acceleration.

To summarize, we make the following contributions:

- We show how modern sparse tensor accelerator features can be represented using cascades of mapped Einsums and primitive operations on fibertrees. Based on this abstraction, we propose the TeAAL specification language for concisely and accurately specifying the architecture of sparse tensor algebra accelerators.
- We propose and design the TeAAL framework for compiling a TeAAL specification into an executable program that can accurately model the specified architecture on real sparse tensor inputs.
- We validate TeAAL’s accuracy with respect to the reported results of four state-of-the-art accelerators.

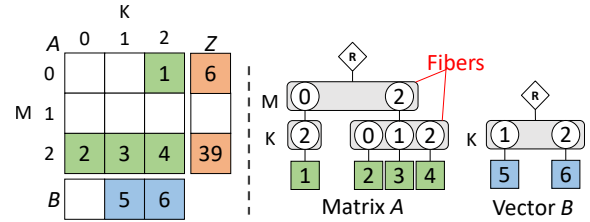


Fig. 1: Sparse matrix-vector multiplication and corresponding fibertree representations.

- We demonstrate the potential of TeAAL as a tool for accelerator design by using it to propose a novel SpMTTKRP accelerator with an average memory traffic reduction of 31% over all prior work.

If accepted, we plan to make TeAAL open source.

II. BACKGROUND AND MOTIVATION

We review key attributes of sparse tensor algebra and outline the design decisions typically made by sparse tensor accelerators when optimizing this computation. We highlight the difficulties with informal comparison between accelerators and motivate the need for a precise, formal specification.

A. Tensors and Fibertrees

In the context of this paper, an N -tensor is a multidimensional array with N dimensions. For example, a 0-tensor is a scalar, a 1-tensor is a vector, and a 2-tensor is a matrix. Figure 1 shows a 2-tensor, A , with dimensions M and K . We use the terminology from [42] to describe the attributes of a tensor:

- A *rank* refers to an axis/dimension in the tensor. A matrix has two ranks: rows and columns.
- A *point* is a specific logical location within a tensor, that contains a scalar *value*. We identify a point by its *coordinates*, an N -tuple with an element for each rank in the tensor. In our notation, we refer to an element of tensor A at point (m, k) as $A_{m,k}$.
- A tensor’s *shape* specifies the domain of values each rank’s coordinates can take. For example, tensor A in Figure 1 has shape $M \times K$, where $M = K = 3$ (i.e., each rank’s coordinate range is $[0, 3)$).

Mathematically, tensors have no notion of sparsity or compression format. To avoid getting bogged down in the numerous details of various formats, we leverage the following abstractions proposed in Sze et al. [42]:

- A *fibertree* represents a tensor as a hierarchical tree, with each level corresponding to a labeled rank in the tensor. Tensor A in Figure 1 has labeled *rank-ids* M and K .
- The order of levels a given tree uses is called its *rank order*, denoted $[M, K]$, and read top-to-bottom in the tree.
- Every level contains one or more *fibers*. A *fiber* is the set of elements sharing all coordinates in all higher levels of the tree. Fibers are more precise than “rows” or “columns,” because they naturally extend to N -tensors.
- Each *element* in the fibertree is a coordinate/payload pair, where the *payload* is a scalar value when it is at a leaf or a reference to a fiber when it is an intermediate node.

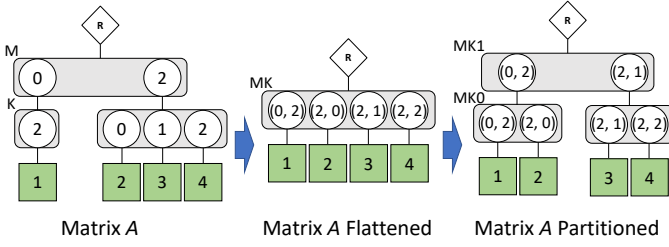


Fig. 2: Flattening/partitioning ranks M and K of tensor A (Fig. 1).

One advantage of fibertrees is that they naturally handle both dense and sparse tensors (i.e., tensors where a number of points contain a zero). A dense tensor’s fibertree has every coordinate present in the entire shape (i.e., a complete tree). On the other hand, a sparse tensor’s fibertree can omit all elements with empty payloads (either zero values or empty fibers). The semantics of operations on fibers and fibertrees remain the same in both cases. In a specific design, all fibertrees are lowered into a concrete in-memory format that may compress the coordinates and/or payloads (see Section IV-A1).

This abstraction also supports a number of transformations that change the fibertree corresponding to a tensor, but do not modify the underlying tensor:

- A *rank swizzle* changes the fibertree’s rank order (i.e., reorders the levels of the fibertree).
- A *rank flattening*, demonstrated in the first transformation in Figure 2, combines two ranks together into a single rank. After flattening, the coordinates are tuples of the coordinates in the original fibers used to reference their corresponding payloads.
- A *rank partitioning*, demonstrated in the second transformation in Figure 2, separates a rank into two ranks. The coordinates of the new upper rank denote the first valid coordinate in the fiber below.

As we will see in Section III, many of the ways that hardware accelerators modify their tensors to improve efficiency can be viewed as one or more of these transformations.

B. Describing Tensor Algebra Using Einstein Summations

For this work, we present an operational definition of an extended Einsum, which specifies the individual computations to occur ([12], [14], [42]). Einsums have been used as the tensor algorithm specification in prior work for tensor algebra compilation [18] and accelerator modeling [30], [48]. An Einsum specifies three things: (1) the input and output tensors involved and their ranks, (2) an *iteration space* relating the ranks together as well as the limits of that space, (3) the computation to be performed at each point in that space. For example, the Einsum for matrix-vector multiply is:

$$Z_m = A_{m,k} \times B_k. \quad (1)$$

Here, the *iteration space*, the Cartesian product of all legal coordinates in the expression, is $M \times K$. An implementation of this Einsum must traverse each point in this space. For each point, it computes the operation (\times) on the right-hand-side using the specified points in the input operands (A, B). It then takes the result and populates the location specified in the

left-hand-side (Z). Since the k variable does not appear in the output tensor, the Einsum implies repeated contributions to the same left-hand-side point (Z_m) via reduction. This reduction is a sum over the rank K for each repeated m —i.e., $\sum_{k=0}^K$. Note that the Einsum does not specify iteration order, this is left to mapping (Section II-C).

By adding a new rank N to B , we can extend the Einsum to matrix multiplication:

$$Z_{m,n} = A_{m,k} \times B_{k,n}. \quad (2)$$

This expands the iteration space to $M \times K \times N$.

C. Mapping Hardware Accelerators

Mapping [7] is the task of scheduling the computation of an Einsum onto limited hardware resources to maximize throughput while minimizing cost (as measured by execution time, energy consumption, etc.). We summarize the mapping attributes used for hardware modeling and design in prior work [6], [15], [16], [20], [26], [30], [49] that we use throughout.

1) Loop order: The Einsum’s large iteration space must be serialized through finite datapath resources in some order. Two choices for Equation 1 are: (1) $[M, K]$ or (2) $[K, M]$. Loop order is read left-to-right, outermost-to-innermost loop. For example, (1) above reads “for each value of m , iterate through all values of k .” This choice affects data locality and, in turn, memory access costs. For example, depending on on-chip buffer sizes, loop order (1) for matrix-vector multiply keeps an element of Z *stationary* [7] in on-chip memory while B is streamed in multiple times. Meanwhile, loop order (2) keeps B stationary but repeatedly streams Z .

2) Partitioning: To further improve data locality across all tensors, many algorithms employ splitting (or tiling, blocking, etc.) to divide the iteration space into subspaces that refer to a small enough subset of each of the tensors that they fit fully in on-chip buffers. In fibertrees, this is represented by *partitioning* all fibers corresponding to that rank across all tensors in the iteration space. How a fiber is partitioned is a function of the coordinates in the fiber. For example, suppose matrix A has a rank-order of $[M, K]$. Splitting K by shape $K0$ results in a new A tensor with shape $[M, K1, K0]$, where K is split into $K1$ tiles each of shape $K0$ in coordinate space.¹

3) Space-time traversal: Finally, the mapping specifies how the iteration space is traversed, by placing each point at a specific location in both time and space. Mapping a computation at different locations in time implies that the computation is serial (i.e., computations happen one after another on the same component), while mapping at different locations in space implies parallelism (i.e., computation happens at the same time on different processing elements (PEs)).

D. Challenges Accelerating Sparse Tensor Algebra

Sparse tensor algebra introduces new opportunities and challenges to the mapping problem. Sparse tensors are typically

¹In other words, each tile stores coordinates in the coordinate range $[i * K0, (i + 1) * K0]$ for some i .

TABLE I: Comparison of selected sparse tensor accelerator hardware proposals. TeAAL specifications increase both the precision and formalism of such comparisons, and enable automatic generation of performance models.

Accelerator	Year	Mapping Approach	Architectural Focus
OuterSPACE [29]	2018	Outer Product parallelized across rows of A	Sparse matrix multiply with serial multiply/add phases, custom merge unit
ExTensor [14]	2019	Inner Product tiled across all dimensions for locality	Arbitrary Einsums and TACO formats [9], skip-ahead intersection unit
MatRaptor [40]	2020	Row-wise Product with parallel summation	Sparse matrix multiply with co-design of micro-architecture and C^2SR format
SIGMA [34]	2020	Inner Product parallelized across multiple dimensions	Sparse matrix multiply with custom bitmap format, flexible hardware topology
SpArch [51]	2020	Outer Product with parallel merge	Sparse matrix multiply with optimized RAM interface in sum phase
Tensaurus [41]	2020	Inner Product with extended scalar-fiber product followed by fiber-fiber product (SF^3)	SF^3 demonstrated applicability to multiple Einsums beyond matrix-matrix multiply
Gamma [50]	2021	Row-wise Product, adoption of Gustavson’s alg.	Sparse matrix multiply with custom FiberCache, transposed merge-and-sum

compressed to remove the zero elements, resulting in fibertrees with missing coordinate-payload pairs. Compression can yield significant savings in storage, data transfers, and compute.

However, realizing these benefits requires accelerators to ‘sparsify’ the iteration space, which increases design complexity, sensitivity to memory latency/bandwidth, and load imbalance. For example, the $[M, K]$ loop order for Equation 1 may move, for example, from $(m = 0, k = 10)$ to $(m = 1, k = 8)$ in a single step. Sparse tensors require *co-iteration* of the operands and additional operations (e.g., intersection for fibers multiplied together) to remove ineffectual compute. Without careful engineering, this can lead to inefficiencies that do not occur when tensors are dense. For example, the same-shape tiles produced by the scheme described in Section II-C may have different memory footprints, leading to data transfer and compute load imbalance when tiles are distributed to workers.

To deal with these challenges, sparse tensor accelerators have proposed a wide variety of custom hardware solutions, summarized in Table I. We note that the complexity of this topic makes such a table an imprecise and ultimately unsatisfying comparison. Additionally, all of these works used custom hand-written simulators of actual data sets to ensure all complexities are captured. In the remainder of this paper we present a formalism to resolve this imprecision and enable concise apples-to-apples comparison. Our framework supports the automatic generation of performance models for a wide range of accelerators, a key savings of engineering effort in the overall design-space exploration process. We think that this approach is extensible, and our framework can easily be modified to support new accelerator features.

III. FRAMEWORK OVERVIEW AND INSIGHTS

This paper proposes TeAAL: a language and toolflow that 1) enables a concise specification of a sparse tensor algebra accelerator architecture and 2) generates efficiency statistics for that accelerator computing on actual sparse tensors.

Our key conceptual contribution, which guides the design of TeAAL, is to show that recent sparse tensor algebra accelerators can be expressed as directed, acyclic graphs (DAGs) of mapped Einsums (Sections II-B, II-C), where computation and data movement (within and across Einsums) is expressed as a small set of primitive operations on fibertrees (Section II-A). This can be articulated as three different, novel insights:

Insight 1: Einsum DAGs can represent multi-phase accelerator designs (Section III-A). We show that DAGs of Einsums are sufficiently expressive to represent computations

broken into multiple disparate phases (e.g., Toeplitz-based convolution, OuterSPACE’s multiply-merge).

Insight 2: Fibertree rank swizzling can represent sort/merge (Section III-B). We show how fibertree rank swizzling is a general pattern for improving tensor traversal efficiency, and manifests as a variety of sorting mechanisms (e.g., the software insertion sort in OuterSPACE and the high-radix hardware merge in Gamma).

Insight 3: Fibertree rank partitioning (and its inverse: flattening) can represent splitting/work distribution (Section III-C). We show how fibertree rank partitioning/flattening is a general pattern for representing both sparse tensor splitting and work-distribution strategies, as a function of the partition criteria (which we define later) and space-time schedule.

Based on the above, accelerators in TeAAL are specified in a declarative, domain-specific language (DSL)—the *TeAAL specification language*. At a high level, TeAAL specifications (in YAML) define the computation as a cascade of Einsums (*expressions*), attributes on each tensor (*declaration, rank-order, partitioning*), and a dataflow that describes when and where those tensors’ data is moved (*loop-order, spacetime*). Rank swizzling is not shown explicitly, but is inferred from other mapping attributes, such as the *rank-order* and *loop-order*. TeAAL represents tensors as fibertrees, and specific accelerators manifest by *lowering* each fibertree to a concrete *format* (e.g., CSR), defining the underlying hardware *architecture*, and *binding* each action (data traffic, compute, etc.) to specific components. The rest of this section details the above three insights, while Section IV discusses the details of the format, architecture, and binding.

OuterSPACE running example. Throughout this section, we use the example TeAAL specification in Figure 3, which describes the OuterSPACE accelerator [29]. At a high level, OuterSPACE accelerates SpMSPM using the *multiply-merge* algorithm. It first performs all multiplications between input tensors A and B in an outer-product fashion, writes resulting partial products to a linked-list log data structure, sorts the linked lists to facilitate reduction, and finally performs said reductions to derive final results. How this is captured (both explicitly and implicitly) in Figure 3 is discussed in the next three sub-sections.

A. Insight 1: Einsum DAGs capture multi-phase accelerators

Our first insight is that seemingly-monolithic tensor algebra kernels (e.g., matrix multiply) are often implemented as a directed acyclic graph of operations, and that each of these operations can often be expressed as Einsums that produce

```

1 einsum:
2   declaration : # Ranks are listed alphabetically in this section.
3   A: [K, M] # Rank order is specified below in rank-order.
4   B: [K, N]
5   T: [K, M, N]
6   Z: [M, N]
7   expressions :
8   - T[k, m, n] = A[k, m] * B[k, n] #  $T_{k,m,n} = A_{k,m} \times B_{k,n}$ 
9   - Z[m, n] = T[k, m, n] #  $Z_{m,n} = T_{k,m,n}$ 
10  mapping:
11  rank-order:
12  A: [K, M]
13  B: [K, N]
14  T: [M, K, N]
15  Z: [M, N]
16  partitioning :
17  T:
18  M:
19  - uniform_occupancy(A.256) # Leader-follower w/ A as leader
20  - uniform_occupancy(A.16)
21  Z:
22  M:
23  - uniform_occupancy(T.128)
24  - uniform_occupancy(T.8)
25  loop-order:
26  T: [K, M2, M1, M0, N] # un-partitioned: [K, M, N]
27  Z: [M2, M1, M0, N, K] # un-partitioned: [M, N, K]
28  spacetime:
29  T:
30  space: [M1, M0]
31  time: [K, M2, N]
32  Z:
33  space: [M1, M0]
34  time: [M2, K, N]

```

Fig. 3: TeAAL specification for the Einsums and mappings of OuterSPACE [29], described in detail in Figure III.

and consume intermediate tensors. For example, consider a 1D convolution between input I and filter F . Convolution is performed using two predominant implementation styles. The first style is direct convolution, which is often employed by accelerators. As an Einsum, direct convolution is written as

$$O_q = I_{q+s} \times F_s \quad (3)$$

An alternative style is the Toeplitz expansion [42], which converts the convolution into a matrix-vector multiply and is common on systolic arrays and data-parallel processors like GPUs. First, the input is refactored into a matrix to enable simple matrix-vector multiplication between the input (now stored in T) and the filter F in the second stage. An important observation is that this can be written as the following sequence of dependent Einsums:

$$T_{q,s} = I_{q+s}; \quad O_q = T_{q,s} \times F_s \quad (4)$$

Importantly, the RHS of the Einsum used to generate T mirrors how I is indexed in the Einsum for direct convolution. The Toeplitz expansion simply relaxes the requirement that the access into I and the corresponding access into F happen at the same time. Note that this sequence of Einsums says nothing about how (if at all) the two stages are overlapped. The entire expansion can happen first and the multiplication second, or the Q rank can be partitioned (Section III-C) and every time a partition of T is produced, it can be consumed by the multiply stage, or any number of other interleavings.

Beyond convolution, DAGs of Einsums can be used to represent other common implementation styles in sparse tensor algebra accelerators. For example, they capture the multiply-and-merge algorithm in the OuterSPACE example (Figure 3). During the multiply phase (Line 8), columns of the A matrix

are multiplied with rows of the B matrix to form partial products, which we call T . Then, during the merge phase, specified by the second Einsum (Line 9), T is reduced along the K rank, yielding the final result Z .

DAGs of Einsums motivate new operations on tensors, and our Einsum notation can be extended to include them if needed. We currently support one—the `take(.)` operator—which decouples intersection from computation with the following semantics: if at least one of the inputs is zero at a point, the output is zero, otherwise, copy one of the inputs into the output. Take the example:

$$T[k,m,n] = \text{take}(A[k,m], B[k,n], 1)$$

The final parameter denotes which input is copied into the output. This example copies B into T , but if the last parameter were 0, A would be copied.

B. Insight 2: Fibertree rank swizzling capture sort/merge

Our second insight is that tensor algebra computations often perform operations that, when expressing their tensors in the fibertree abstraction, are tantamount to fibertree rank swizzles. These operations enable the more efficient *concordant* (as opposed to *discordant* [42]) traversal. Concordant traversal occurs when a loop nest traverses a fibertree in the order in which its ranks appear, i.e., traverses each fiber sequentially and in a depth-first manner. For example, matrices A and B in Figure 3 are traversed concordantly. For simplicity, assume the loop order sans partitioning (given in the comments on Lines 26-27). K is the outer-most rank in both the rank and loop orders for the multiply stage (Lines 12-13, 26), and M and N appear as inner ranks. Thus, we never have to search for the next m or n coordinate, it is always either the first or next coordinate in the current fiber(s). Conversely, iterating over K in the inner-most loop would be a discordant traversal (for this rank order).

It is common practice to swizzle ranks to enable concordant traversal on input tensors. For example, the CSC format can be viewed as a rank swizzle of a matrix stored in the CSR format, and is used by OuterSPACE to achieve a $[K, M]$ rank order on A (Line 12) in preparation for the outer-product-style multiply phase. Input tensor swizzles are usually performed offline.

More subtly, we observe that sparse tensor accelerators also perform rank swizzles on *intermediate tensors* formed during kernels expressed as DAGs of Einsums (Section III-A). Depending on whether coordinates in the intermediate tensors are stored in sorted or unsorted order and on the extent to which the intermediate tensors are built before being consumed, this either requires a merge or a (more expensive) sort operation.

Figure 4 shows an example of a multiply-merge for outer product, matrix-vector multiplication. To support concordant traversal on both input and output tensors, the multiply phase uses a $[K, M]$ loop order, while the merge phase uses an $[M, K]$ loop order. Thus, at the end of the multiply phase, T has rank order $[K, M]$. Then, during the reduction, a rank swap changes the rank order of T to $[M, K]$ to match the $[M, K]$ loop order. The dashed arrows in Figure 4 show that *both*

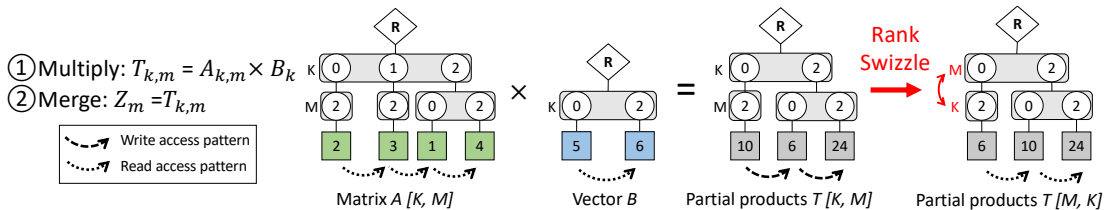


Fig. 4: Rank swizzling in sparse tensor algebra computations, using outer-product multiply-merge matrix-vector multiplication. Matrix A and vector B use values from Figure 1 for consistency. An offline rank swap ensures that A has rank order $[K, M]$ prior to the multiply phase, and an online rank swap ensures that T has rank order $[M, K]$ prior to the merge phase, ensuring concordant traversal in both phases.

the tensor read and write access patterns through A , B and T are all concordant through both phases. Importantly, such online rank swaps may degrade performance, and therefore warrant dedicated hardware support. Yet, they can significantly improve spatial/temporal locality, and thus, appear in multiple prior designs [29], [50], [51].

By default, rank swizzles in TeAAL are inferred automatically to maintain concordant traversal through all fibertrees in all Einsums. For example, for OuterSPACE (Figure 3), even though the rank order for T is $[M, K, N]$, the TeAAL framework produces T during the multiply phase in $[K, M, N]$ order, swizzles it to $[M, K, N]$ order to be stored in memory, and then swizzles it again to $[M, N, K]$ order to prepare for the merge. TeAAL also supports expressing other (e.g., discordant) traversals through explicit mapping directives.

C. Insight 3: Fibertree rank partitioning/flattening capture splitting/work distribution

Our third insight is that fibertree rank partitioning (and its inverse: flattening) can be used as a single abstraction for specifying both sparse tensor splitting and work distribution strategies. Note that, though all partitioning directives modify the fibertree abstract representation, the concrete representation may remain unchanged.

1) *Sparse Tensor Splitting*: Recall from Section II-C, the splitting for dense problems is shape-based. This can be expressed by partitioning a fibertree rank at coordinate-based boundaries given by the tile dimension. Unfortunately, this strategy can lead to under-utilization of tiles (and therefore buffers) [14] and lower reuse when data is sparse, i.e., if different partitions have different occupancies.

A key observation is that partitioning naturally generalizes to other types of splitting that *can* adapt to irregular sparsity, simply by changing the *partitioning criteria*, i.e., where the partition boundaries occur. From studying existing accelerators, we define a simple sparsity-aware strategy here, which we call *uniform occupancy-based partitioning*. In this scheme, each fiber at a level in the fibertree is split so that each new fiber has an equal number of elements (modulo remainders).

Importantly, each fiber’s coordinate range after an occupancy-based partitioning is irregular. Thus, to ensure that partitions of multiple tensors have matching coordinate ranges for co-iteration (Section II-C), occupancy-based partitioning uses a *leader-follower* paradigm: the partitions’ coordinate ranges are chosen so that the leader tensor’s partitions are equal occupancy and all follower tensors adopt those ranges.

TABLE II: Supported hardware components and their attributes.

Component	Attributes
DRAM	bandwidth
Buffer	type (buffer [32] or cache), width, depth, bandwidth
Intersection	type (two-finger, leader-follower, or skip-ahead), leader
Merger	inputs, comparator_radix, outputs, order (fifo, opt), reduce
Compute	type (mul or add)

2) *Sparse Work Distribution*: More subtly, we observe that partitioning is also a useful abstraction through which to specify work distribution strategies when work is parallelized. Consider the OuterSPACE example, which works on 256 non-empty elements of matrix A at a time during the multiply phase, and further sub-divides these into 16 groups of 16 elements to each be processed by a so-called “Processing Tile” (a group of PEs [29]). The TeAAL specification for OuterSPACE (Figure 3) represents these on Lines 19-20 as occupancy-based partitioning applied twice hierarchically, with the A tensor leading the partitioning.²

Unfortunately, occupancy-based partitioning may still result in partitions with uneven data footprints because a partition must end where its parent fiber ends. However, flattening (Section II-A), when combined with occupancy-based partitioning, mitigates this data imbalance by first combining all ranks, and then redistributing the elements so that globally each partition has the same number of values. For example, Figure 2 shows how a fibertree whose two partitions start with an unequal number of coordinates can be flattened and re-partitioned to equalize the number of coordinates per partition.

IV. GENERATING THE PERFORMANCE MODEL

In Section III, we showed that the fibertree abstraction is general enough to describe many of the design decisions used in sparse tensor accelerators. However, to manifest a specific design, the fibertrees must be lowered onto concrete representations and their operations bound to specific hardware components. In this section, we define three additional specifications—*format*, *architecture*, and *binding*—used by TeAAL to perform this lowering, and describe how these plus the *einsum* and *mapping* specifications from Section III are combined to produce an executable model for evaluating accelerator workload performance.

A. Specifications to Lower Mapped Einsums to Hardware

1) *Format*: Prior works on modeling sparse tensor algebra computations [9], [42], [48] propose a convenient abstraction

²Note: OuterSPACE only enables half of its PEs during the merge step. Hence the occupancy-based partitioning applied to the second Einsum (Lines 23-24) only involves 128 PEs (8 per “Processing Tile”).

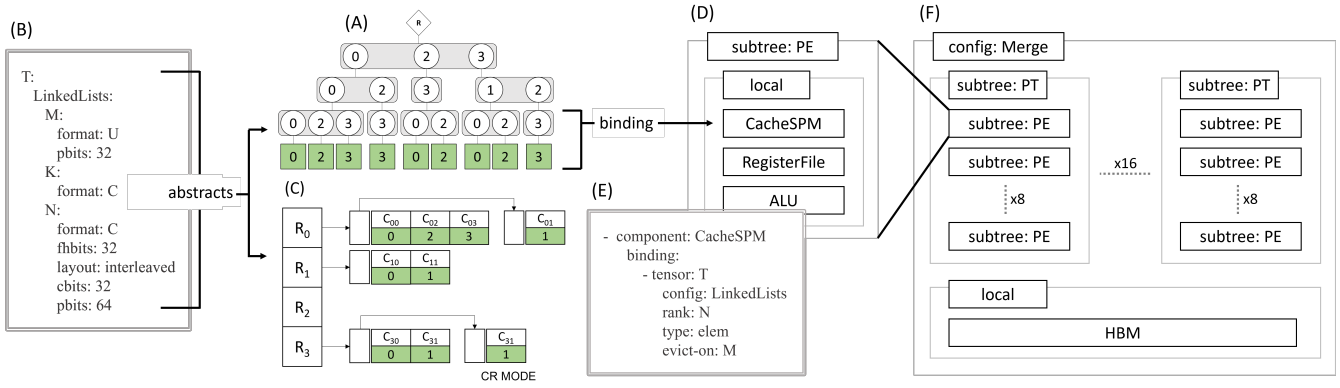


Fig. 5: TeAAL concrete/hardware-level model of the OuterSPACE accelerator [29].

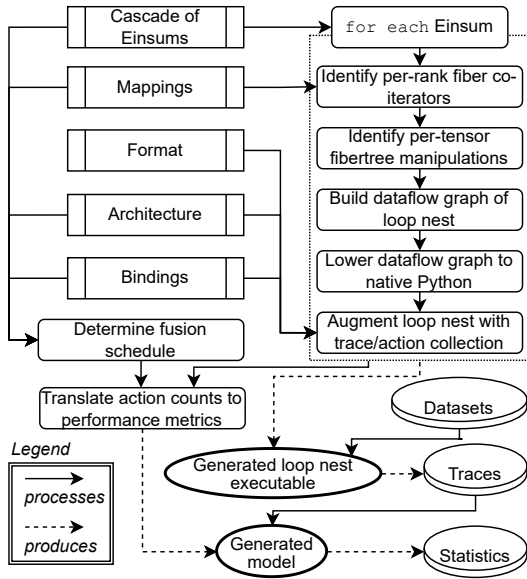


Fig. 6: TeAAL tool flow diagram, described in detail in Section IV-C.

for translating a fibertree to the actual data footprint: a per-fiber format. However, the formats used by existing sparse accelerator modeling frameworks restrict themselves to a fixed number of common configurations (e.g., bitmap [27] or uncompressed offset pointers [48]).

TeAAL enables more modular specification, capturing a larger class of formats than existing tools, by separating the attributes of a fiber’s format into three categories: a format type, a layout, and data widths for the coordinates, payloads, and fiber header. TeAAL supports three format types: uncompressed (U)—where the sizes of the data arrays correspond to the shape of the fiber, compressed (C)—where the sizes of the data arrays correspond to the occupancy of the fiber, or a combination (B)—where the coordinates are uncompressed and the payloads are compressed. For simplicity, currently, all fibers in a rank have the same format.

Note that some of the information associated with the fibertree can be stored implicitly by assigning that metadata no corresponding data width, e.g. an uncompressed fiber does not need to explicitly store coordinates. This specification is flexible enough to support a wide variety of common formats

(e.g., dense arrays and CSR) and custom formats (e.g., from OuterSPACE [29] and SIGMA [34]). TeAAL also supports multiple formats for the same tensor (specified by unique configuration names), since manipulating the fibertree may cause the representation to change dynamically.

2) *Architecture*: The TeAAL architecture specification (inspired by Timeloop [30]) describes the accelerator topology as a tree of compute and storage units. At each level of the hierarchy, one can define a list of hardware components local to that level and a list of subtrees below that level. In addition to the component classes supported by Timeloop [30], we define new classes of components that are involved in performance-limiting operations on sparse accelerators, including caches, intersection units, and hardware mergers. Table II gives the full list of supported classes and their attributes. Since an accelerator (e.g., OuterSPACE [29]) may reorganize itself during the execution of a single computation, TeAAL also supports specifying multiple topologies for the same design.

3) *Binding*: Finally, TeAAL’s binding specification matches the Einsum- and mapping-induced fibertree operations to specific concrete representations and hardware components. First, each Einsum must be bound to a single accelerator topology. Then, for each storage component, the binding describes what data resides there—as specified by its tensor, configuration, rank, and type (e.g., payload)—and sometimes (e.g., for buffers [32]), for how long. Similarly, for each compute component, the binding describes which compute operations are performed on that component.

B. Modeling OuterSPACE [29]

We continue to use OuterSPACE as a running example to motivate the features provided by the TeAAL framework. For brevity, Figure 5 shows a simplified version of OuterSPACE’s custom tensor format, its architecture during the merge phase, and the correspondence between the fibertree representation of T and its concrete representation and binding. In Figure 5A, we see the fibertree for an example tensor T . The format specification (Figure 5B) for this tensor lowers it onto OuterSPACE’s custom array of linked lists format (Figure 5C). To differentiate it from other representations of the same tensor, we give it the configuration name *LinkedLists*. On the M rank, the array of pointers is given by an uncompressed (U)

array of payloads. On the N rank, the fiber header data width (*fhbits*) describes the linked list pointers, the *layout* describes that corresponding coordinates and payloads are adjacent, and the *cbits* and *pbits* describe the data widths of the coordinates and payloads, respectively.

Figure 5D shows an OuterSPACE PE. During the merge phase, this level has three local components: the L0 scratchpad, the register file, and the ALU. OuterSPACE loads the entire subtree under a given M coordinate into the L0 scratchpad to perform its software sort. TeAAL expresses this binding with the following specification given in Figure 5E. The *tensor*, *config*, *rank*, and *type* denote exactly what data is buffered, and the *evict-on* keyword is required for binding to explicitly managed buffers, whose fill and drain policy must be set by the user. Because the elements bound to this buffer evict on M , old data is drained when the M coordinate changes. Finally, Figure 5F shows an overview of the entire accelerator topology.

C. TeAAL Framework, Model, and Modeling Philosophy

Figure 6 demonstrates how TeAAL puts everything together. For each Einsum, TeAAL combines the equation with its mapping information to identify the necessary per-tensor fibertree manipulations (e.g., rank swizzling) and per-rank fiber co-iterators (e.g., intersection). Using this information, it builds a dataflow graph of the loop nest, which it then lowers to an embedded, domain-specific language within Python for executing computation as fibertree operations [1].

The TeAAL framework breaks the modeling of an accelerator into two stages. First, the loop nests perform the computation on fibertrees and generate a trace of when each coordinate and each payload is accessed. Then, a model processes those traces to generate statistics that describe the accelerator’s performance characteristics. In this work, we compute statistics with a bottleneck analysis. We identify five crucial bottlenecks in sparse tensor algebra accelerator performance: multiplication, addition, intersection, rank swizzling, and data movement. These operations are tallied for each component at the level of individual operations (e.g., cache hits and misses, intersection tests, etc.). The model then determines the performance of each Einsum using the performance of the slowest component. Note that this is just one option for the implementation of the model. The traces generated by the loop nest have enough information to produce a higher fidelity model that accounts for the added latencies due to dependencies between components, though we leave its implementation to future work.

The format, architecture, and binding together specify the desired traces, allowing TeAAL to augment the loop nest to collect those traces. TeAAL provides a library of per-component models, which it adds calls to after the loop nest to translate the traces to action counts. These action counts can be passed to a power model, such as Accelergy [46], to compute energy use.

Separately, the full cascade of Einsums, mappings, architectures, and bindings are used to determine the extent to which

individual Einsums are fused together, i.e., their computation is overlapped (see Section III-A). TeAAL infers that Einsums can be fused together when three conditions are met:

- The Einsums use the same accelerator configuration.
- The temporal ranks in all loop orders before the first spatial rank are the same.
- All non-storage components are exclusively used by only one Einsum.

As a simple heuristic, it greedily fuses Einsums together into a single block, trying to minimize the number of Einsum blocks. Based on this fusion schedule, TeAAL translates the outputs of the per-component models into performance metrics.

TeAAL evaluates its model using real datasets. It loads the tensors as fibertrees and executes the generated loop nests on those fibertrees, producing traces of fibertree operations and accesses. These traces are fed to the model, which produces both the individual per-Einsum, per-component action counts and an estimate of the overall performance.

V. SPECIFYING STATE-OF-THE-ART ACCELERATORS

Sections III-IV used OuterSPACE [29] as a running example. We now describe the Einsums and mapping specifications for three other accelerators relevant to our evaluation, shown in Figure 7. We omit the format/architecture/bindings for brevity.

A. Gamma [50]

Gamma (Figure 7a) is a row-wise Gustavson’s style accelerator that uses a tightly-pipelined multiply and merge style architecture to reduce partial output traffic and enable concordant traversal across both input and output tensors. Gamma’s overall architecture is made up of PEs that connect with a global shared FiberCache which connects to main memory.

In Gustavson’s dataflow, a row of A is combined and reduced with rows of B . Gamma distributes rows of A to each PE and, based on which values in each row are non-zero, the PE fetches a subset of the rows of B . This filtering is implemented using the `take(.)` operator (Section III-A). After being fetched to each PE, the rows of B (which initially have rank order $[K, N]$) are sorted with hardware mergers to facilitate reduction over K . Similar to OuterSPACE, this is expressed as a rank swap: T has rank order $[M, K, N]$ and the rightmost (innermost) rank in the loop order for the Einsum computing Z is K . Hence, the compiler inserts a rank swap on T , making its rank order in the context of the second Einsum $[M, N, K]$. Unlike OuterSPACE, multiply and merge in Gamma is done in a tightly-coupled fashion: immediately after rows of B are loaded to PEs, they are merged and reduced along K , with partial outputs buffered and re-fetched as needed from the FiberCache. This is expressed in the loop order and spacetime schedule. Note that the spacetime schedules for the T and Z Einsums are the same, except that the N and K ranks are swapped.

```

1 einsum:
2 declaration :
3 A: [K, M]
4 B: [K, N]
5 T: [K, M, N]
6 Z: [M, N]
7 expressions :
8 - T[k,m,n] = take(A[k,m], B[k,n], 1)
9 - Z[m,n] = T[k,m,n]*A[k,m]
10 mapping:
11 rank-order:
12 A: [M, K]
13 B: [K, N]
14 T: [M, K, N]
15 Z: [M, N]
16 partitioning :
17 T:
18 M: [uniform_occupancy(A.32)]
19 K: [uniform_occupancy(A.64)]
20 Z:
21 M: [uniform_occupancy(A.32)]
22 K: [uniform_occupancy(A.64)]
23 loop-order:
24 T: [M1, M0, K1, K0, N]
25 Z: [M1, M0, K1, N, K0]
26 spacetime:
27 T:
28 space: [M0, K1]
29 time: [M1, K0, N]
30 Z:
31 space: [M0, K1]
32 time: [M1, N, K0]

```

(a) Gamma accelerator [50].

```

1 einsum:
2 declaration :
3 A: [K, M]
4 B: [K, N]
5 Z: [M, N]
6 expressions :
7 - Z[m,n] = A[k,m] * B[k,n]
8 mapping:
9 rank-order:
10 A: [K, M]
11 B: [K, N]
12 Z: [M, N]
13 partitioning :
14 Z:
15 K:
16 - uniform_shape(K1)
17 - uniform_shape(K0)
18 M:
19 - uniform_shape(M1)
20 - uniform_shape(M0)
21 N:
22 - uniform_shape(N1)
23 - uniform_shape(N0)
24 loop-order:
25 Z: [N2, K2, M2, M1, N1, K1, M0, N0, K0]
26 spacetime:
27 Z:
28 space: [K1]
29 time: [N2, K2, M2, M1, N1, M0, N0, K0]

```

(b) ExTensor accelerator [14].

```

1 einsum:
2 declaration :
3 A: [K, M]
4 B: [K, N]
5 T: [K, M]
6 Z: [M, N]
7 expressions :
8 - T[k, m] = take(A[k, m], B[k, n], 0)
9 - Z[m, n] = T[k, m] * B[k, n]
10 mapping:
11 rank-order:
12 A: [K, M]
13 B: [K, N]
14 T: [K, M]
15 Z: [M, N]
16 partitioning :
17 Z:
18 K: [uniform_shape(128)]
19 (M, K0): [flatten 0]
20 MK0: [uniform_occupancy(T.16384)]
21 loop-order:
22 T: [K, M]
23 Z: [K1, MK01, N, MK00]
24 spacetime:
25 T:
26 space: []
27 time: [K, M]
28 Z:
29 space: [MK00]
30 time: [K1, MK01, M]

```

(c) SIGMA accelerator [34].

Fig. 7: State-of-the-art sparse tensor accelerators. `uniform_shape()` and `flatten()` are syntax for TeAAL’s shape-based partitioning and flattening directives (Section III-C), respectively.

B. ExTensor [14]

ExTensor (Figure 7b) employs a hybrid dataflow that is inner product-style at the innermost level, keeping distinct tensors stationary at distinct levels. The overall architecture is made up of PEs, which connect to a shared global buffer, which connects to main memory.

ExTensor’s two salient characteristics are the use of uniform shape-based partitioning (Section II-C) and hierarchical intersection. Uniform-shape partitions are loaded into the global buffer, then broken down into sub-tiles and distributed to PEs (expressed by parallelizing over the $K1$ rank). Hierarchical intersection is accounted for implicitly due to fibertree semantics (Section II-D). Note that our ExTensor specification includes additional details beyond the original paper, from private correspondence with the authors about the actual decisions made in the simulator used for evaluation.

C. SIGMA [34]

SIGMA (Figure 7c) is a flexible deep-learning accelerator that uses occupancy-based partitioning to reduce ineffectual computation. SIGMA uses an occupancy-based partitioning to only distribute non-zero elements of the stationary matrix to PEs, removing all multiply-accumulates on zero elements of that matrix. While the SIGMA architecture can be configured to support both A and B -stationary dataflows, we only describe and evaluate the A -stationary dataflow here.

SIGMA utilizes a pipeline of Einsums (Section III-A) to reduce ineffectual computation by first removing all K -fibers (columns) of A that correspond to empty K -fibers (rows) in B (Line 8), then performing the multiplication (Line 9). We express the partitioning using a combination of shape-based partitioning, flattening, and occupancy-based partitioning (Section III-C2). First, in Line 18, a shape-based partitioning splits the K rank so that each $K0$ -fiber (partition of a row) of B

TABLE III: Tensor data set characteristics.

Matrix	Shape	NNZ	Domain
wiki-Vote (wi)	$8.3K \times 8.3K$	104K	elections
p2p-Gnutella31 (p2)	$63K \times 63K$	148K	file-sharing
ca-CondMat (ca)	$23K \times 23K$	187K	collab. net.
poisson3Da (po)	$14K \times 23K$	353K	fluid dynamics
email-Enron (em)	$37K \times 37K$	368K	email comms.
chicago-crime (ch)	$6.1K \times 77 \times 32$	2.75M	crime counts
nips (ni)	$2.5K \times 14K \times 2.9K$	3.1M	word counts
uber (ub)	$1.1K \times 1.7K \times 183$	1.1M	pickup counts

TABLE IV: Hardware configs, chosen to match original publications.

ExTensor [14]	1 GHz clock speed, 128 PEs, 64 kB PE buffer per PE, 30 MB LLC, 68.256 GB/s memory bandwidth
Gamma [50]	1 GHz clock speed, 64-way merger per PE, 32 PEs, 3 MB Fiber-Cache, 16 64-bit HBM channels, 8 GB/s/channel
OuterSPACE [29]	1.5 GHz clock speed, 16 PEs per PT, 16 PTs, 16 kB L0 cache per PT, 4 kB L1 cache per 4 PTs, 16 64-bit HBM channels, 8000 MB/s/channel
SIGMA [34]	500 MHz clock speed, 128 PEs per FlexDPE, 128 FlexDPEs, 32 MB Data SRAM, 4 MB Bitmap SRAM, 960 GB/s SRAM bandwidth, 1024 GB/s HBM bandwidth
Tensaurus [41]	2 GHz clock speed, 8×8 PE array, 544 KB SRAM, 128 GB/s memory bandwidth

can be distributed in a single cycle in the worst case. Then, all elements of the A matrix that will be multiplied by a given fiber of B are flattened together (Line 19) and, on Line 20, re-partitioned with an occupancy-based partitioning equal to the number of PEs, minimizing inactive PEs during the computation. Finally, because all PEs work in parallel, the spatial dimension is $MK00$ (Line 29).

VI. EVALUATION

A. Methodology

Tensors. To validate TeAAL on the accelerators described in Figures 3, 5, and 7, we evaluate each accelerator on a combination of randomly generated matrices with uniform sparsity and a set of matrices from SuiteSparse [10] and SNAP [22]. To evaluate existing SpMTTKRP designs and our novel dataflow, we use three 4-tensors from FROSTT [37].

For each 4-tensor, we flattened together two of the ranks to create 3-tensors, and then used TensorSketch sampling [33] to reduce the shape of the flattened rank down to the larger of the two original ranks (needed to increase the density to allow tensor decomposition to actually compress the tensors). The details can be found in Table III.

Simulation Framework. We implement each of the four accelerators by writing TeAAL specifications for their Einsums, mappings, formats, architectures and bindings. For each accelerator, we use the hardware parameters given in Table IV. TeAAL uses Accelry [46] as a power model to convert the per-component action counts to an energy characterization.

Baselines. To validate our results, we normalize our performance estimates using the same baseline as the original papers that published the relevant accelerators. All accelerators’ “reported” statistics come either from published results or from private communication with the original authors. When possible, we also report Sparseloop [48] performance estimates using the *hypergeometric* sparsity distribution on both the inputs and outputs, estimated using the values in Table III, and the hardware parameters in Table IV.

B. Simulator Validation

In this section, we describe a set of experiments used to validate TeAAL as an accurate cost model. Specifically, we compare memory traffic and performance as reported by TeAAL to the numbers reported in the papers originally proposing each accelerator.

Memory Traffic. Figure 8 presents a comparison of the memory traffic of the TeAAL models of each of accelerators to the corresponding baseline. The takeaway is that we can reproduce each accelerator’s memory traffic with low error (on average, 3.8%).

Performance. Figure 9 presents a performance comparison of each TeAAL model against the reported numbers and Sparseloop [48]’s estimate, when possible. Figure 9a compares the speedup of ExTensor over Intel MKL according to the original simulator, the TeAAL model, and a Sparseloop model on the same set of real-world matrices. TeAAL shows consistently low error rates (on average, 12%). Sparseloop has an average error of 63%, which we attribute to its analytical sparsity distribution. Sparseloop first performs dense modeling and then applies its sparse analysis. We could not model p2 because the sizes of the dense tensors caused an integer overflow error. We were also unable to use Sparseloop to model Gamma or OuterSPACE (because it does not support cascades of Einsums) or SIGMA (because its occupancy-based partitioning is not sufficiently general). Figure 9b compares the speedup of Gamma over Intel MKL for the set of real-world matrices on both the original simulator and the TeAAL cost model. Our work shows very similar results to the original paper: an average error of only 6.2%. Because we could not obtain the raw baseline used in the OuterSPACE paper, Figure 9c shows the performance of the original simulator and the TeAAL model on a number of uniformly sparse synthetic matrices. On average, our cost model is about 80% faster

than the original simulator, though the overall trend is consistent. Prior works [29], [51] contain different estimates for OuterSPACE’s performance, even on the same benchmarks, making it impossible to establish a ground-truth and root-cause the discrepancy. Finally, Figure 9d compares the speedup of SIGMA over the Google Cloud TPU on a set of randomly generated matrices. For this experiment, all A matrices had 80% sparsity and all B matrices had 10% sparsity. Here, we show an average error of only 2.8%.

Energy. Figure 10 compares TeAAL’s energy estimates to the reported baseline, showing consistently low error rates—on average, 7.8%. Since none of the other accelerators reported their per-component, per-action energy consumption characteristics, we were unable to validate the power model on those designs.

C. Design of Novel Accelerators: SpMTTKRP

In this section, we demonstrate the value of TeAAL as a framework for designing and evaluating new sparse tensor algebra accelerators. As an example, we perform an analysis of proposed mappings for the SpMTTKRP kernel, and use our insights to propose a novel mapping.

Sparse Matricized Tensor Times Khatri-Rao Product (SpMTTKRP) is the key computational kernel used to perform the sparse canonical polyadic decomposition (CPD) [41], [44], a technique for decomposing an $I \times J \times K$ sparse tensor into three dense matrices of shapes $I \times R$, $J \times R$, and $K \times R$ respectively. The Einsum for MTTKRP looks like: $C_{i,r} = T_{i,j,k} B_{j,r} A_{k,r}$. We can also rewrite MTTKRP as cascaded Einsums:

$$S_{i,j,r} = T_{i,j,k} A_{k,r} \quad C_{i,r} = S_{i,j,r} B_{j,r}$$

We start with a set of three candidate accelerators based on prior work: a Tensaurus [41]-like design (which uses the single Einsum), a Wijeratne et al. [44]-like design³ (which uses the cascaded Einsums), and a Choi et al. [8]-like design (which uses the cascaded Einsums and partitions the R rank). We evaluate each accelerator on three benchmark tensors (see Table III) and three values of R^4 : 4, 32, and 128. To perform an apples-to-apples comparison, we use the hardware characteristics of the Tensaurus accelerator (see Table IV).

The memory traffic incurred in the algorithmic minimum and by the three candidate designs, found in Figure 11, reveals that neither of the cascaded Einsum accelerators provide a significant improvement over the Tensaurus-like design. Since all experiments except one (Tensaurus-like, $R = 32$, on ub) were memory bound, the cost of the additional memory traffic is not out-weighed by the benefit gained from performing less compute.

We use these results to design a better accelerator, as modeled by TeAAL. All three configurations incurred significant memory traffic on A , so we would like our proposal improve

³This dataflow is also used in the popular SPLATT library [38].

⁴ R is an independent variable that trades of compression for accuracy. A smaller value of R results in a more compressed, but more inaccurate decomposition.

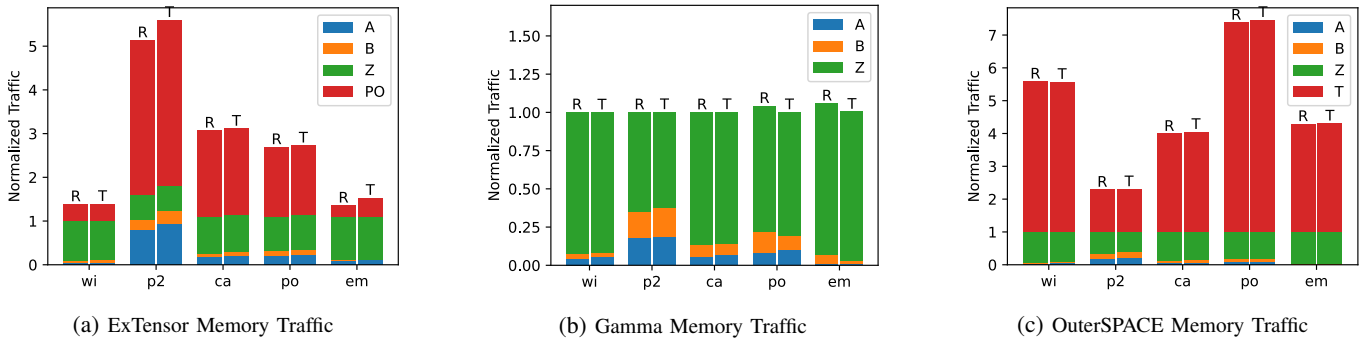


Fig. 8: Comparison of the memory traffic reported by the original authors (left) and the TeAAL model (right) for ExTensor, Gamma, and OuterSPACE on each of the 5 real-world tensors, normalized to the algorithmic minimum traffic. Benchmark acronyms are defined in Table III. Tensor names A , B , T , and Z correspond to the names defined in the Einsums in Figures 3 and 7. PO denotes the partial outputs (i.e. Z traffic that is not the final write of Z).

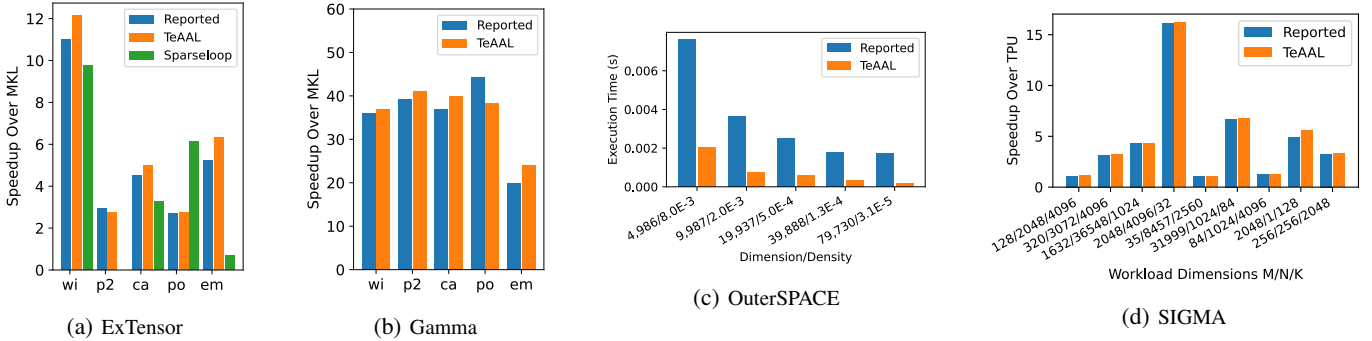


Fig. 9: Validation of TeAAL-generated timing models against original publications. Benchmark acronyms in Table III.

TABLE V: Sparse tensor modeling frameworks.

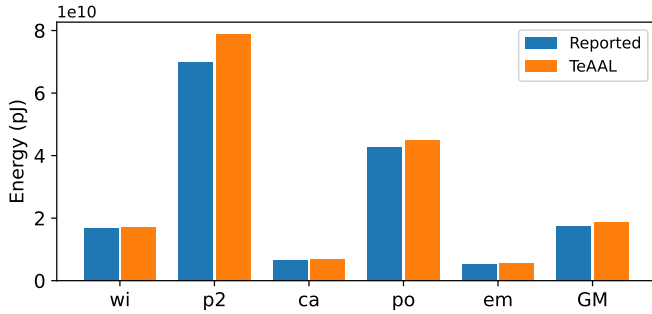


Fig. 10: Validation of the ExTensor energy model. Benchmark acronyms can be found in Table III.

the locality on this matrix. We are especially interested in improving experiments with a large R value, since these incur traffic many more times above the algorithmic minimum. Additionally, we see from the Wijeratne et al.-like accelerator that streaming over T can detrimentally increase the memory traffic in some cases (all three experiments on ch). Therefore, we propose a novel design that improves reuse of A and keeps T stationary via shape-based partitioning all four ranks.

This configuration (marked new) decreases memory traffic by an average of 14% across all benchmarks by improving reuse of A while keeping the memory traffic associated with T , B , and C low. We attribute the poor performance of our proposal on ni to its extremely low density (3.1×10^{-5}), which causes our shape-based partitions to not capture very much reuse. These experiments also point to the benefits of

	STONNE [27]	CIN-P [2]	Sparse-loop [48]	TeAAL (this work)
Precise Data Set	✓			✓
Generic Computations		✓	✓	✓
Shape-Based Partitioning			✓	✓
Occ-Based Partitioning				✓
Flattening			✓	✓
Rank Swizzling		✓		✓
Caches				✓
Cascaded Einsums		✓		✓
Format Expressivity		✓	✓	✓

flexible dataflow architectures, which can choose different configurations dynamically based on the input data [21], [23]. An accelerator that can execute our proposed mapping, with and without partitioning, would achieve an average 31% decrease in memory traffic. Further improvement may come from splitting our proposal into cascaded Einsums (since four of the nine configurations are now compute bound) or applying a Gamma-like preprocessing step (to improve locality).

VII. RELATED WORK

The rise in machine learning and tensor algebra accelerators has been followed by an increase in tools exploring the accelerator design space and modeling performance and costs [2], [16], [19], [20], [26], [27], [30], [36], [47], [49]. The lion share of the frameworks solely support dense computations and target DNN applications [16], [20], [26], [30].

Table V compares frameworks that model architectures computing on sparse tensors. STONNE [27] is a cycle-level

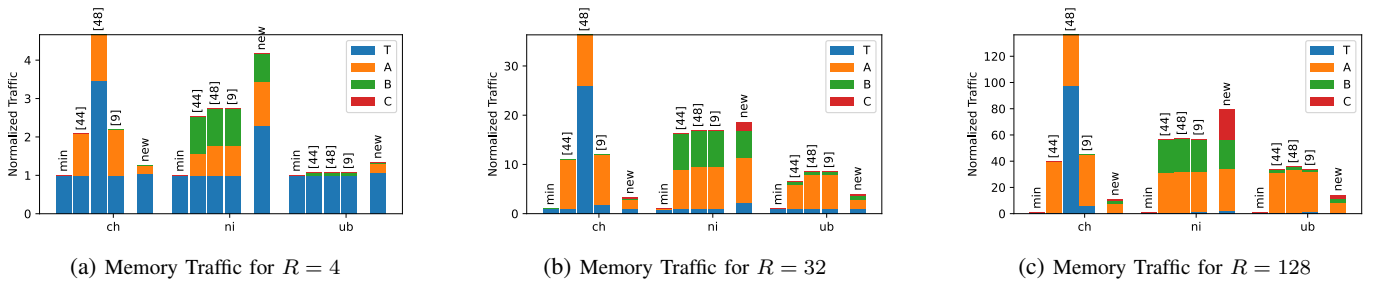


Fig. 11: Comparison of the memory traffic of different accelerators running MTTKRP: the algorithmic minimum (min), Tensaurus-like ([41]), Wijeratne et al.-like ([44]), Choi et al.-like ([8]), and our proposal (new), as modeled by TeAAL. All configurations use the hardware parameters given for Tensaurus in Tabel IV.

modeling framework for DNN accelerators. Like TeAAL, STONNE’s analysis is data-driven; however, the only sparse workload it supports is SpMSPM. CIN-P [2] is a mapper language that, when combined with an asymptotic cost model and autoscheduler, generates mappings that can then be compiled using TACO [19]. Since it uses asymptotic analysis, the mapper only considers loop order, loop fusion, and rank swizzling transformations. However, it does not consider partitioning and architectural features like caches or parallel units. Sparseloop, on the other hand, has a flexible hardware backend and takes as input a specification of the architecture, a statistical model of the data, sparse optimizations such as skip-based intersection [14], and a user-specified mapping. It returns estimates of performance and energy consumption. Unlike TeAAL, it does not support many of the mapping features important to sparse computations, such as cascaded Einsums, caches, rank swizzling, and others. Additionally, CIN-P and Sparseloop analytically model the tensors’ sparsity patterns. The data-driven nature of TeAAL enables cost estimates that better reflect the specific distribution of a given workload.

VIII. CONCLUSION

This paper presents TeAAL: a framework for describing and evaluating sparse tensor accelerators. The key contribution is to demonstrate how state-of-the-art sparse accelerators can be represented as cascades of mapped Einsums and primitive operations on fibertrees. From this observation, we propose the TeAAL language which enables designers to utilize and combine these concepts (for both the modeling of current and design of new accelerators), and a compiler from this language to executable simulators that emulate fibertree operations (lowered onto concrete data representations and hardware units).

In the long term, we anticipate TeAAL will enable a more efficient accelerator design process supported by quantitative reasoning, while providing the architecture community with a common language for comparing and discussing designs. Also, while the current TeAAL framework backend generates performance models, we think other backends (e.g., for generating hardware directly) are possible.

REFERENCES

[1] , “Redacted for anonymous submission,” -.

- [2] P. Ahrens, F. Kjolstad, and S. P. Amarasinghe, “Autoscheduling for sparse tensor algebra with an asymptotic cost model,” in *PLDI ’22: 43rd ACM SIGPLAN International Conference on Programming Language Design and Implementation, San Diego, CA, USA, June 13 - 17, 2022*. ACM, 2022, pp. 269–285. [Online]. Available: <https://doi.org/10.1145/3519939.3523442>
- [3] H. M. Aktulga, A. Buluç, S. Williams, and C. Yang, “Optimizing sparse matrix-multiple vectors multiplication for nuclear configuration interaction calculations,” in *IPDPS’14*, 2014.
- [4] J. Albericio, P. Judd, T. H. Hetherington, T. M. Aamodt, N. D. E. Jerger, and A. Moshovos, “Cnvlutin: Ineffectual-neuron-free deep neural network computing,” in *43rd ACM/IEEE Annual International Symposium on Computer Architecture, ISCA 2016, Seoul, South Korea, June 18-22, 2016*. IEEE Computer Society, 2016, pp. 1–13. [Online]. Available: <https://doi.org/10.1109/ISCA.2016.11>
- [5] A. Azad, A. Buluç, and J. Gilbert, “Parallel triangle counting and enumeration using matrix algebra,” in *IPDPS’15 Workshop*, 2015.
- [6] T. Chen, T. Moreau, Z. Jiang, H. Shen, E. Q. Yan, L. Wang, Y. Hu, L. Ceze, C. Guestrin, and A. Krishnamurthy, “TVM: end-to-end optimization stack for deep learning,” *CoRR*, vol. abs/1802.04799, 2018. [Online]. Available: <http://arxiv.org/abs/1802.04799>
- [7] Y.-H. Chen, J. Emer, and V. Sze, “Eyeriss: A spatial architecture for energy-efficient dataflow for convolutional neural networks,” ser. ISCA’16.
- [8] J. Choi, X. Liu, S. Smith, and T. Simon, “Blocking optimization techniques for sparse tensor computation,” in *2018 IEEE International Parallel and Distributed Processing Symposium (IPDPS)*, 2018, pp. 568–577.
- [9] S. Chou, F. Kjolstad, and S. Amarasinghe, “Format abstraction for sparse tensor algebra compilers,” *Proc. ACM Program. Lang.*, vol. 2, no. OOPSLA, pp. 123:1–123:30, Oct. 2018. [Online]. Available: <http://doi.acm.org/10.1145/3276493>
- [10] T. A. Davis and Y. Hu, “The university of florida sparse matrix collection,” *ACM Trans. Math. Softw.*, vol. 38, no. 1, dec 2011. [Online]. Available: <https://doi.org/10.1145/2049662.2049663>
- [11] S. Dongen, “Graph clustering by flow simulation,” *PhD thesis, Center for Math and Computer Science (CWI)*, 05 2000.
- [12] A. Einstein, “The foundation of the general theory of relativity,” *Annalen der Physik*, vol. 354, no. 7, pp. 769–822, Jan. 1916.
- [13] S. Han, X. Liu, H. Mao, J. Pu, A. Pedram, M. A. Horowitz, and W. J. Dally, “Eie: efficient inference engine on compressed deep neural network,” in *ISCA’16*.
- [14] K. Hegde, H. Asghari-Moghaddam, M. Pellauer, N. Crago, A. Jaleel, E. Solomonik, J. Emer, and C. W. Fletcher, “ExTensor: An Accelerator for Sparse Tensor Algebra,” in *MICRO’19*.
- [15] K. Hegde, P.-A. Tsai, S. Huang, V. Chandra, A. Parashar, and C. W. Fletcher, “Mind Mappings: Enabling Efficient Algorithm-Accelerator Mapping Space Search,” in *ASPLOS’21*.
- [16] Q. Huang, M. Kang, G. Dinh, T. Norrell, A. Kalaiah, J. Demmel, J. Wawrzynek, and Y. S. Shao, “Cosa: Scheduling by constrained optimization for spatial accelerators,” *2021 ACM/IEEE 48th Annual International Symposium on Computer Architecture (ISCA)*, pp. 554–566, 2021.
- [17] J. Hutter, M. Iannuzzi, F. Schiffmann, and J. VandeVondele, “cp2k: atomistic simulations of condensed matter systems,” *WIREs Computational Molecular Science*, vol. 4, no. 1, pp. 15–25, 2014. [Online]. Available: <https://wires.onlinelibrary.wiley.com/doi/abs/10.1002/wcms.1159>

- [18] F. Kjolstad, S. Kamil, S. Chou, D. Lugato, and S. Amarasinghe, “The tensor algebra compiler,” *Proceedings of the ACM on Programming Languages*, vol. 1, no. OOPSLA, pp. 77:1–77:29, Oct. 2017.
- [19] F. Kjolstad, S. Kamil, S. Chou, D. Lugato, and S. Amarasinghe, “The tensor algebra compiler,” *Proc. ACM Program. Lang.*, vol. 1, no. OOPSLA, oct 2017. [Online]. Available: <https://doi.org/10.1145/3133901>
- [20] H. Kwon, M. Pellauer, and T. Krishna, “Maestro: An open-source infrastructure for modeling dataflows within deep learning accelerators,” *ArXiv*, vol. abs/1805.02566, 2018.
- [21] H. Kwon, A. Samajdar, and T. Krishna, “Maeri: Enabling flexible dataflow mapping over dnn accelerators via reconfigurable interconnects,” *SIGPLAN Not.*, vol. 53, no. 2, pp. 461–475, Mar. 2018. [Online]. Available: <http://doi.acm.org/10.1145/3296957.3173176>
- [22] J. Leskovec and A. Krevl, “SNAP Datasets: Stanford large network dataset collection,” <http://snap.stanford.edu/data>, Jun. 2014.
- [23] W. Lu, G. Yan, J. Li, S. Gong, Y. Han, and X. Li, “Flexflow: A flexible dataflow accelerator architecture for convolutional neural networks,” in *HPCA’17*.
- [24] M. Mahmoud, I. Edo, A. H. Zadeh, O. M. Awad, G. Pekhimenko, J. Albericio, and A. Moshovos, “Tensordash: Exploiting sparsity to accelerate deep neural network training,” in *53rd Annual IEEE/ACM International Symposium on Microarchitecture, MICRO 2020, Athens, Greece, October 17-21, 2020*. IEEE, 2020, pp. 781–795. [Online]. Available: <https://doi.org/10.1109/MICRO50266.2020.00069>
- [25] T. Mattson, D. Bader, J. Berry, A. Buluc, J. Dongarra, C. Faloutsos, J. Feo, J. Gilbert, J. Gonzalez, B. Hendrickson, J. Kepner, C. Leiserson, A. Lumsdaine, D. Padua, S. Poole, S. Reinhardt, M. Stonebraker, S. Wallach, and A. Yoo, “Standards for graph algorithm primitives,” in *HPEC’13*, 2013.
- [26] L. Mei, P. Houshmand, V. Jain, S. Giraldo, and M. Verhelst, “Zigzag: A memory-centric rapid dnn accelerator design space exploration framework,” 2020.
- [27] F. Muñoz-Martínez, J. L. Abellán, M. E. Acacio, and T. Krishna, “Stonne: Enabling cycle-level microarchitectural simulation for dnn inference accelerators,” *IEEE Computer Architecture Letters*, vol. 20, no. 2, pp. 122–125, 2021.
- [28] Y. Nagasaka, S. Matsuoka, A. Azad, and A. Buluc, “Performance optimization, modeling and analysis of sparse matrix-matrix products on multi-core and many-core processors,” *Parallel Computing*, vol. 90, p. 102545, Dec. 2019.
- [29] S. Pal, J. Beaumont, D.-H. Park, A. Amarnath, S. Feng, C. Chakrabarti, H.-S. Kim, D. Blaauw, T. Mudge, and R. Dreslinski, “Outerspace: An outer product based sparse matrix multiplication accelerator,” 02 2018, pp. 724–736.
- [30] A. Parashar, P. Raina, Y. S. Shao, Y.-H. Chen, V. A. Ying, A. Mukkara, R. Venkatesan, B. Khailany, S. W. Keckler, and J. Emer, “Timeloop: A systematic approach to dnn accelerator evaluation,” in *2019 IEEE International Symposium on Performance Analysis of Systems and Software (ISPASS)*, 2019, pp. 304–315.
- [31] A. Parashar, M. Rhu, A. Mukkara, A. Puglielli, R. Venkatesan, B. Khailany, J. Emer, S. W. Keckler, and W. J. Dally, “Scnn: An accelerator for compressed-sparse convolutional neural networks,” in *ISCA’17*.
- [32] M. Pellauer, Y. Shao, J. Clemons, N. Crago, K. Hegde, R. Venkatesan, S. Keckler, C. Fletcher, and J. Emer, “Buffets: An Efficient and Composable Storage Idiom for Explicit Decoupled Data Orchestration,” in *ASPLOS’19*.
- [33] N. Pham and R. Pagh, “Fast and scalable polynomial kernels via explicit feature maps,” in *Proceedings of the 19th ACM SIGKDD International Conference on Knowledge Discovery and Data Mining*, ser. KDD ’13. New York, NY, USA: Association for Computing Machinery, 2013, p. 239–247. [Online]. Available: <https://doi.org/10.1145/2487575.2487591>
- [34] E. Qin, A. Samajdar, H. Kwon, V. Nadella, S. Srinivasan, D. Das, B. Kaul, and T. Krishna, “Sigma: A sparse and irregular gemm accelerator with flexible interconnects for dnn training,” in *2020 IEEE International Symposium on High Performance Computer Architecture (HPCA)*, 2020, pp. 58–70.
- [35] J. Ragan-Kelley, C. Barnes, A. Adams, S. Paris, F. Durand, and S. Amarasinghe, “Halide: A language and compiler for optimizing parallelism, locality, and recomputation in image processing pipelines,” *SIGPLAN Not.*, vol. 48, no. 6, p. 519–530, jun 2013. [Online]. Available: <https://doi.org/10.1145/2499370.2462176>
- [36] R. Senanayake, C. Hong, Z. Wang, A. Wilson, S. Chou, S. Kamil, S. Amarasinghe, and F. Kjolstad, “A sparse iteration space transformation framework for sparse tensor algebra,” *Proc. ACM Program. Lang.*, vol. 4, no. OOPSLA, Nov. 2020. [Online]. Available: <https://doi.org/10.1145/3428226>
- [37] S. Smith, J. W. Choi, J. Li, R. Vuduc, J. Park, X. Liu, and G. Karypis. (2017) FROSTT: The formidable repository of open sparse tensors and tools. [Online]. Available: <http://frostt.io/>
- [38] S. Smith, N. Ravindran, N. D. Sidiropoulos, and G. Karypis, “Splatt: Efficient and parallel sparse tensor-matrix multiplication,” in *2015 IEEE International Parallel and Distributed Processing Symposium*, 2015, pp. 61–70.
- [39] E. Solomonik, M. Besta, F. Vella, and T. Hoefer, “Scaling betweenness centrality using communication-efficient sparse matrix multiplication,” in *Proceedings of the International Conference for High Performance Computing, Networking, Storage and Analysis*, 2017.
- [40] N. Srivastava, H. Jin, J. Liu, D. Albonesi, and Z. Zhang, “Matraprot: A sparse-sparse matrix multiplication accelerator based on row-wise product,” in *2020 53rd Annual IEEE/ACM International Symposium on Microarchitecture (MICRO)*, 2020, pp. 766–780.
- [41] N. Srivastava, H. Jin, S. Smith, H. Rong, D. Albonesi, and Z. Zhang, “Tensaurus: A versatile accelerator for mixed sparse-dense tensor computations,” in *2020 IEEE International Symposium on High Performance Computer Architecture (HPCA)*, 2020, pp. 689–702.
- [42] V. Sze, Y. Chen, T. Yang, and J. S. Emer, *Efficient Processing of Deep Neural Networks*, ser. Synthesis Lectures on Computer Architecture. Morgan & Claypool Publishers, 2020. [Online]. Available: <https://doi.org/10.2200/S01004ED1V01Y202004CAC050>
- [43] J. VandeVondele, U. Borštnik, and J. Hutter, “Linear scaling self-consistent field calculations with millions of atoms in the condensed phase,” *Journal of Chemical Theory and Computation*, vol. 8, no. 10, pp. 3565–3573, 2012, pMID: 26593003. [Online]. Available: <https://doi.org/10.1021/ct200897x>
- [44] S. Wijeratne, R. Kannan, and V. Prasanna, “Reconfigurable low-latency memory system for sparse matricized tensor times khatri-rao product on fpga,” 2021. [Online]. Available: <https://arxiv.org/abs/2109.08874>
- [45] J. Wilhelm, P. Seewald, M. Del Ben, and J. Hutter, “Large-scale cubic-scaling random phase approximation correlation energy calculations using a gaussian basis,” *Journal of Chemical Theory and Computation*, vol. 12, no. 12, pp. 5851–5859, 2016, pMID: 27779863. [Online]. Available: <https://doi.org/10.1021/acs.jctc.6b00840>
- [46] Y. N. Wu, J. S. Emer, and V. Sze, “Accelergy: An architecture-level energy estimation methodology for accelerator designs,” in *2019 IEEE/ACM International Conference on Computer-Aided Design (ICCAD)*, 2019, pp. 1–8.
- [47] Y. N. Wu, P.-A. Tsai, A. Parashar, V. Sze, and J. S. Emer, “Sparseloop: An analytical, energy-focused design space exploration methodology for sparse tensor accelerators,” in *2021 IEEE International Symposium on Performance Analysis of Systems and Software (ISPASS)*, 2021, pp. 232–234.
- [48] Y. N. Wu, P.-A. Tsai, A. Parashar, V. Sze, and J. S. Emer, “Sparseloop: An analytical approach to sparse tensor accelerator modeling,” *2022 55th IEEE/ACM International Symposium on Microarchitecture (MICRO)*, pp. 1377–1395, 2022.
- [49] X. Yang, M. Gao, Q. Liu, J. Setter, J. Pu, A. Nayak, S. Bell, K. Cao, H. Ha, P. Raina, C. Kozyrakis, and M. Horowitz, “Interstellar: Using halide’s scheduling language to analyze dnn accelerators,” in *Proceedings of the Twenty-Fifth International Conference on Architectural Support for Programming Languages and Operating Systems*, ser. ASPLOS ’20. New York, NY, USA: Association for Computing Machinery, 2020, p. 369–383. [Online]. Available: <https://doi.org/10.1145/3373376.3378514>
- [50] G. Zhang, N. Attaluri, J. S. Emer, and D. Sanchez, “Gamma: Leveraging gustavson’s algorithm to accelerate sparse matrix multiplication,” in *Proceedings of the 26th ACM International Conference on Architectural Support for Programming Languages and Operating Systems*, ser. ASPLOS 2021, 2021, pp. 687–701. [Online]. Available: <https://doi.org/10.1145/3445814.3446702>
- [51] Z. Zhang, H. Wang, S. Han, and W. J. Dally, “Sparch: Efficient architecture for sparse matrix multiplication,” in *26th IEEE International Symposium on High Performance Computer Architecture (HPCA)*, 2020.